Eylem Demircioglu[1]
Aysun Sofuoglu[2]
Mustafa Odabasi[1]

[1]Faculty of Engineering, Department of Environmental Engineering, Dokuz Eylul University, Izmir, Turkey
[2]Faculty of Engineering, Department of Chemical Engineering, Izmir Institute of Technology, Gulbahce-Urla, Turkey

Research Article

Atmospheric Concentrations and Phase Partitioning of Polycyclic Aromatic Hydrocarbons in Izmir, Turkey

Ambient air polycyclic aromatic hydrocarbon (PAH) samples were collected at a sub-urban ($n = 63$) and at an urban site ($n = 14$) in Izmir, Turkey. Average gas-phase total PAH ($\sum_{14}$PAH) concentrations were 23.5 ng m^{-3} for suburban and 109.7 ng m^{-3} for urban sites while average particle-phase total PAH concentrations were 12.3 and 34.5 ng m^{-3} for suburban and urban sites, respectively. Higher ambient PAH concentrations were measured in the gas-phase and $\sum_{14}$PAH concentrations were dominated by lower molecular weight PAHs. Multiple linear regression analysis indicated that the meteorological parameters were effective on ambient PAH concentrations. Emission sources of particle-phase PAHs were investigated using a diagnostic plot of fluorene (FLN)/(fluorine + pyrene; PY) versus indeno[1,2,3-cd]PY/(indeno[1,2,3-cd]PY + benzo[g,h,i]perylene) and several diagnostic ratios. These approaches have indicated that traffic emissions (petroleum combustion) were the dominant PAH sources at both sites for summer and winter seasons. Experimental gas–particle partition coefficients (K_P) were compared to the predictions of octanol–air (K_{OA}) and soot–air (K_{SA}) partition coefficient models. The correlations between experimental and modeled K_P values were significant ($r^2 = 0.79$ and 0.94 for suburban and urban sites, respectively, $p < 0.01$). Octanol-based absorptive partitioning model predicted lower partition coefficients especially for relatively volatile PAHs. However, overall there was a relatively good agreement between the measured K_P and soot-based model predictions.

1 Introduction

Polycyclic aromatic hydrocarbons (PAHs) are a complex class of organic compounds containing two or more fused aromatic rings, and only carbon and hydrogen. PAHs are formed as a result of incomplete combustion and released into the environment through natural and anthropogenic sources. There are hundreds of individual PAHs in the environment, however, only 16 PAH compounds have been classified by the U.S. Environmental Protection Agency (USEPA) as priority pollutants [1]. At ambient temperatures, PAHs are solids. The general characteristics common to the class are high melting- and boiling-points, low vapor pressure, and very low water solubility [2].

Atmospheric PAHs are distributed between gas and particle-phases. The partitioning of PAHs between the gas and particle-phases is an important factor affecting their removal processes [2, 3]. PAHs are removed from the atmosphere by transformation, wet and dry deposition, air–water exchange, and air–soil exchange.

Atmospheric levels of PAHs have been widely measured around the world [4–15]. Despite their environmental relevance, only a few studies have been conducted in Turkey on the atmospheric PAH levels [14–19]. The objectives of this study were to investigate (1) the ambient air concentrations of 14 PAHs and their temporal variations in Izmir, Turkey, (2) the effect of meteorological parameters on ambient concentrations, (3) the possible sources of PAHs in the study area, and (4) their gas/particle partitioning.

2 Materials and methods

2.1 Sampling program and collection

Ambient air samples were collected at two sampling sites (suburban and urban) in Izmir (Fig. 1). The suburban samples were collected on a 4-m high platform located on the Kaynaklar Campus of the Dokuz Eylul University, ∼10 km southeast of Izmir's center. This site is relatively far from any settlement zones or industrial facilities.

Correspondence: Dr. A. Sofuoglu, Faculty of Engineering, Department of Chemical Engineering, Izmir Institute of Technology, 35430 Gulbahce-Urla, Turkey
E-mail: aysunsofuoglu@iyte.edu.tr

Abbreviations: ANT, anthracene; **BaA**, benz[*a*]anthracene; **BaP**, benzo[*a*]pyrene; **BbF**, benzo[*b*]fluoranthene; **BghiP**, benzo[*g,h,i*]perylene; **BkF**, benzo[*k*]fluoranthene; **CHR**, chrysene; **CRB**, carbazole; **DahA**, dibenzo[*a,h*]anthracene; **FL**, fluoranthene; **FLN**, fluorene; **IcdP**, indeno[1,2,3-*cd*]pyrene; **MLR**, multiple linear regression; **OM**, organic matter; **PAH**, polycyclic aromatic hydrocarbon; **PHE**, phenanthrene; **PUF**, polyurethane foam; **PY**, pyrene; **TSP**, total suspended particles.
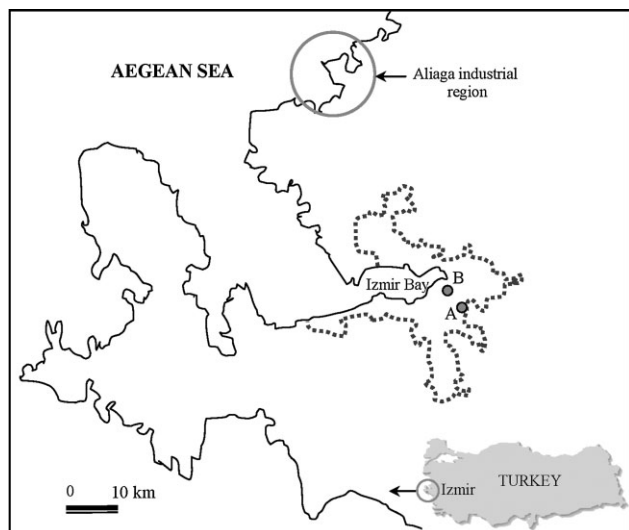
Figure 1. Map of the Izmir showing the sampling sites. (A) Suburban sampling site, (B) Urban sampling site. Dashed line is border of densely populated areas.

There are residential areas located approximately 2 km southwest and a highway located 0.5 km south of the sampling site. Land cover in the immediate area is a young coniferous forest. There are steel plants, a petroleum refinery, and petrochemical industry located 45 km to the northwest. The nearest industrial facility is a cement work about 10 km at north and an open road gravel storage site nearly 3 km at the east. Urban samples were collected from Yesildere site located near a main street with heavy traffic and residential areas.

Sixty-three ambient air samples were collected between May 2003 and May 2004 at the suburban site. Another two additional sampling campaigns were conducted between March 17–24, 2004 (winter) and July 15–22, 2004 (summer) at the urban site. Successive seven ambient air samples were collected for each sampling period. All samples were collected when there was no rain. Samples were also collected to determine the total suspended particles (TSP) and their organic matter (OM) content. Meteorological data were obtained from a 10-m high tower located at the suburban sampling site.

Air samples were collected using a modified high-volume sampler model GPS-11 (Thermo-Andersen Inc.). Particles were collected on 10.5-cm diameter quartz filters and the gas-phase compounds were collected in a modified cartridge containing XAD-2 resin placed between layers of polyurethane foam (PUF). Concurrently, particle samples were collected on 11-cm diameter glass fiber filters using another high-volume sampler to determine TSP and its OM content. The average sampling volumes for PAHs were 173 ± 44 and $277 \pm 62 \, m^3$ and the average sampling volume for TSP were 40.5 ± 8.5 and $93.9 \pm 13.0 \, m^3$ at suburban and urban sites, respectively. Sampling time ranged between 11 h (suburban) and 22 h (urban).

Prior to sampling, quartz filters were baked at 450°C overnight. Then, they were allowed to cool to room temperature in a desiccator. PUF cartridges (two PUF plugs + XAD-2 resin layer) were cleaned by Soxhlet extraction using an acetone/hexane mixture (1:1) for 12 h, dried in an oven at 70°C, and stored in glass jars capped with Teflon-lined lids. After sampling, PS-1 filters and PUF cartridges were stored at −20°C in their containers.

2.2 Sample preparation and analysis

Ambient air samples (filters and PUF cartridges) were separately Soxhlet extracted for 12 h with a mixture of 20:80 dichloromethane (DCM):petroleum ether (PE). Prior to extraction, all samples were spiked with PAH surrogate standards (naphthalene-d8, acenaphthene-d10, phenanthrene (PHE)-d10, chrysene-d12, and perylene-d12) to monitor the analytical recovery efficiencies. The extract volumes were reduced and the solvent was exchanged into hexane using a rotary evaporator and a high-purity N_2 stream. After concentrating to 2 mL, samples were cleaned up and fractionated on an alumina–silicic acid column containing 3 g of silicic acid (deactivated with 3% deionized water) and 2 g of alumina (deactivated with 6% deionized water). The column was pre-washed with 20 mL of DCM followed by 20 mL of PE. Then, the sample in 2 mL hexane was added to the column and PAHs were eluted with 20 mL DCM. The final extracts were solvent exchanged into hexane and concentrated to 1 mL under a stream of N_2.

Prior to sampling for TSP, baked and cooled glass fiber filters were weighed using a microbalance capable of weighing 0.1 mg. After collection of sample, they were kept in a desiccator overnight and reweighed. TSP was obtained by subtracting the initial weight from the final weight. OM contents of the particles were determined by subtracting the filters baked in a furnace for 1 h at 450°C from the initial weight before baking.

All samples were analyzed for 14 PAHs including fluorene (FLN), PHE, anthracene (ANT), carbazole (CRB), fluoranthene (FL), pyrene (PY), benz[*a*]anthracene (BaA), chrysene (CHR), benzo[*b*]fluoranthene (BbF), benzo[*k*]fluoranthene (BkF), benzo[*a*]pyrene (BaP), indeno[1,2,3-*cd*]pyrene (IcdP), dibenzo[*a,h*]anthracene (DahA), and benzo[*g,h,i*]perylene (BghiP) with an Agilent 6890N GC equipped with a mass selective detector (Agilent 5973 inert MSD). A capillary column (HP5-ms, 30 m, 0.25 mm, 0.25 μm) was used. The initial oven temperature was held at 50°C for 1 min and raised to 200°C at 25°C min^{-1}, 200–300°C at 8°C min^{-1}, and was held for 5.5 min. The injector, ion source, and quadrupole temperatures were 295, 300, and 180°C, respectively. High-purity helium was used as the carrier gas at constant flow mode (1.5 mL min^{-1}). The MSD was run in selected ion-monitoring mode. All compounds were identified based on their retention times, target, and qualifiers ions. The quantification was based on internal standard calibration procedure.

2.3 Quality control

Average recoveries of PAH surrogate standards were $68 \pm 14\%$ for PHE-d10 ($n = 147$), $82 \pm 14\%$ for CHR-d12 ($n = 154$), and $77 \pm 19\%$ for perylene-d12 ($n = 152$) for all ambient air samples. The recoveries of target compounds were also tested by matrix spiking experiments and average recovery efficiencies were between $88 \pm 22\%$ (DahA) and $121 \pm 6\%$ (IcdP) (overall average $\pm$ SD, $107 \pm 16\%$).

Blank PUF cartridges and air filters were routinely placed in the field to determine if there was any contamination during sampling, sample handling, and preparation. PHE had the highest amount in blanks with an average of 123 ± 43 ng for PUFs and 79 ± 21 ng for air filters. Average blank amounts for PUFs and air filters were 11 ± 10 and $8 \pm 13\%$ of the sample amounts for all analyzed PAHs, respectively. Instrumental detection limits (IDL) were determined from linear extrapolation from the lowest standard in calibration curve using the area of a peak having a signal/noise ratio of 3. The quantifiable PAH amount was approximately 0.15 pg for 1 μL injection. IDL

was used for the compounds that were not detected in blanks. The limit of detection of the method (LOD) was defined as the mean blank mass plus three standard deviations. LODs for 14 PAH compounds ranged from 2 ng (BaP) to 253 ng (PHE) for PUFs and 2 ng (BaA) to 143 ng (PHE) for PS-1 filters. These values correspond to air concentrations of 0.01 ng m^{-3} (BaP) to 0.9 ng m^{-3} (PHE) for PUFs, and 0.01 ng m^{-3} (BaA) to 0.5 ng m^{-3} (PHE) for PS-1 filters. Sample quantities exceeding the LOD were quantified and blank-corrected by subtracting the mean blank amount from the sample amount for all samples.

Six levels of calibration standards (0.04, 0.4, 1.0, 4.0, 6.0, and 10.0 μg mL^{-1}) were used to calibrate the GC/MS system. In all cases, the r^2 of the calibration curve was ≥0.999. System performance was verified by the analysis of the mid-point calibration standard for every 24 h during the analysis period.

Concurrent blank filters were run for each TSP and OM sample to determine if there was any contamination during sample handling and preparation, and to account for probable interferences (i.e., weight loss of filters at high temperatures) in OM determination. The average weight loss of blank filters (0.38 mg) was significantly lower than the average weight loss of the samples (2.5 mg) indicating that the interference was not significant in OM determination.

3 Results and discussion

3.1 Ambient PAH concentrations

Gas and particle-phase concentrations of individual PAHs at all sites are presented in Tab. 1. Average gas-phase total PAH ($\sum_{14}$PAH) concentrations were 23.5 ng m^{-3} for suburban and 109.7 ng m^{-3} for urban sites while average particle-phase total PAH concentrations were 12.3 and 34.5 ng m^{-3} for suburban and urban sites, respectively. Measured average total (gas + particle) PAH concentrations were 36 ± 39 and 144 ± 163 ng m^{-3} for suburban and urban sites in this study. The concentrations of PAHs may have a diurnal variation. This may be a confounding factor for the comparison of

Table 1. Ambient air concentrations (ng m^{-3}) of individual PAHs for suburban and urban sites (average ± SD)

PAHs	Suburban		Urban	
	Gas	Particle	Gas	Particle
FLN	4.1 ± 4.5	0.6 ± 1.0	12.5 ± 10.3	0.1 ± 0.1
PHE	11.7 ± 12.1	1.9 ± 2.6	40.8 ± 36.2	1.0 ± 0.8
ANT	0.5 ± 0.7	0.1 ± 0.1	5.6 ± 6.2	0.1 ± 0.1
CRB	0.4 ± 0.8	0.2 ± 0.3	1.0 ± 2.0	0.1 ± 0.1
FL	3.7 ± 4.1	1.5 ± 2.5	27.3 ± 43.5	2.8 ± 3.7
PY	2.4 ± 2.4	1.4 ± 2.2	20.2 ± 27.0	3.1 ± 4.2
BaA	0.1 ± 0.1	0.5 ± 1.0	0.6 ± 0.5	3.0 ± 4.8
CHR	0.4 ± 0.3	1.5 ± 2.5	1.6 ± 1.0	6.2 ± 8.6
BbF	0.05 ± 0.04	0.9 ± 1.3	0.03 ± 0.02	3.4 ± 4.1
BkF	0.02 ± 0.01	0.8 ± 1.2	0.02 ± 0.01	3.6 ± 4.6
BaP	0.02 ± 0.02	0.7 ± 1.0	0.008 ± 0.006	3.1 ± 4.7
IcdP	0.01 ± 0.01	0.9 ± 1.4	0.006 ± 0.004	3.4 ± 4.5
DahA	0.02 ± 0.03	0.4 ± 0.7	0.003 ± 0.001	1.3 ± 1.9
BghiP	0.03 ± 0.04	0.9 ± 1.1	0.008 ± 0.005	3.4 ± 3.8
$\sum_{14}$ PAH	23.5 ± 23.8	12.3 ± 16.2	109.7 ± 111.7	34.5 ± 45.7

the measurement results from the urban site (for 22 h) and suburban site (for 11 h). The values measured in the present study were within the range of previously reported values in other urban and industrial sites around the world (Tab. 2). Total $\sum_{14}$PAH concentrations measured at the suburban, and urban sites in the present study are considerably lower than those reported for urban sites in Bursa [14] and in Chicago [5] while they are significantly higher than those reported for urban Athens [8]. The PAH levels measured at the suburban site in this study are similar to those reported for an industrial site in Izmir, for urban Heraklion, for industrial sites in Fuji and Shimizu, and for urban/industrial Baltimore (Tab. 2).

The gas/particle phase distributions indicated that about 69 and 81% of $\sum_{14}$PAHs were in the gas-phase for the suburban and urban sites, respectively. Because of their higher volatility, low to medium molecular weight PAHs (3−5 rings) were more abundant in the gas-phase similar to the previous studies [10, 14, 20, 21].

Table 2. Total PAH concentrations ($\sum_n$ PAH, ng m^{-3}) measured around the world

Location	Number of PAHs included in $\sum$PAH (n)	Industrial	Urban	Suburban/ Rural	References
Taichung, Taiwan	13	678.7	476.7	319.4[a]	[21]
Chicago, USA	13		351.8		[5]
Bursa, Turkey	13	224.6			[14]
Rome, Italy	12		162.4		[12]
London, UK	11		160.6		[4]
Stevenage, UK	11	90.3			[4]
Seoul, Korea	13		67.3		[9]
Heraklion, Greece	12		51.5		[13]
Fuji, Japan	13	46			[10]
Baltimore, USA	13		24		[6]
Athens, Greece	10	15.4			[8]
New Jersey, USA	10		27.5		[7]
Izmir, Turkey	14	43.5			[15]
Zonguldak, Turkey	14		298		[16]
Konya, Turkey	16		206		[17]
Bursa, Turkey	15		298		[18]
Bursa, Turkey	14		152[b]–1249[c]		[19]
Izmir, Turkey	14		144	36	

[a] Rural area.
[b] Non-heating season.
[c] Heating season.

Table 3. Summary of regression parameters for Eq. (1) for all sites and individual compounds

	m_1	m_2	m_3	r^2	n
Suburban					
FLN	−0.28[a]	−0.51[a]	0.60	0.26	63
PHE	−0.71[a]	−1.53[a]	2.39	0.24	63
ANT	−0.05[a]	−0.04	0.06	0.31	63
CRB	0.00	0.03	0.08	0.01	63
FL	−0.39[a]	−0.42	0.67	0.25	63
PY	−0.28[a]	−0.41	0.64	0.28	63
BaA	−0.06[a]	−0.08	0.14	0.28	63
CHR	−0.16[a]	−0.26[a]	0.40	0.26	63
BbF	−0.07[a]	−0.13[a]	0.22	0.25	63
BkF	−0.07[a]	−0.12[a]	0.20	0.27	63
BaP	−0.05[a]	−0.11[a]	0.20	0.23	63
IcdP	−0.06[a]	−0.17[a]	0.32	0.19	63
DahA	−0.02	−0.12[a]	0.29[a]	0.24	63
BghiP	−0.05[a]	−0.16[a]	0.30	0.22	63
Urban					
FLN	−0.27	−4.70[a]	3.68	0.62	14
PHE	−0.14	−20.38[a]	15.68	0.67	14
ANT	−0.41	−2.79[a]	4.48[a]	0.82	14
CRB	−0.05	−0.98[a]	1.57	0.54	14
FL	−3.00	−16.70	39.11[a]	0.63	14
PY	−1.89	−12.03[a]	26.03[a]	0.67	14
BaA	−0.25	−2.49[a]	4.34[a]	0.76	14
CHR	−0.47	−4.45[a]	7.08[a]	0.78	14
BbF	−0.20	−1.91[a]	2.70[a]	0.74	14
BkF	−0.24	−2.08[a]	3.27[a]	0.74	14
BaP	−0.22	−2.21[a]	3.91[a]	0.75	14
IcdP	−0.17	−2.27[a]	3.16[a]	0.75	14
DahA	−0.06	−0.94[a]	1.33[a]	0.72	14
BghiP	−0.16	−1.80[a]	2.44[a]	0.73	14

[a] $p < 0.05$.

In the suburban site, PHE, FLN, FL, and PY accounted for 42, 14, 12, and 10% of Σ_{14} PAHs in summer period while in urban site they were 41, 12, 14, and 15% of Σ_{14} PAHs. During winter, the contributions of PHE, FLN, FL, and PY in suburban and urban sites were 35, 12, 16, and 11%, 26, 8, 22, and 16% of Σ_{14} PAHs, respectively. These percentages were similar to those reported previously [5, 15, 20].

3.2 Effect of meteorological parameters on gas-phase PAH concentrations

The effect of wind speed and direction on atmospheric concentrations of individual PAHs was investigated using multiple linear regression (MLR) analysis [22]:

$$C_t = m_1 T + m_2 U + m_3 \cos WD + b \tag{1}$$

where C_t is the total (gas + particle phase) PAH concentration (ng m^{-3}), T the average atmospheric temperature (°C), U the wind speed (m s^{-1}), WD the predominant wind direction (radians) during the sampling period, and m_1–m_3, and b are the regression parameters.

The results of MLR analysis are presented in Tab. 3. Temperature, wind speed, and wind direction together accounted for 1% (CRB) to 31% (ANT), and 54% (CRB) to 82% (ANT) of the variability in the atmospheric PAH concentrations for suburban and urban sites, respectively. The m_1 values were insignificant for all PAHs for urban site. The m_1 values were statistically significant for all PAHs ($p < 0.05$) except CRB and DahA for suburban site. Generally negative m_1 values

were obtained for PAHs indicated that their concentrations increased with decreasing temperature. This was probably due to increased PAH emissions from combustion sources like residential heating with decreased ambient temperature. For most of the compounds, m_2 had negative values and they were statistically significant for most of the compounds. This indicated that their concentrations decreased as the wind speed increased and advection was also an important parameter controlling the concentrations of atmospheric PAHs. Negative values for m_3 indicate that relatively higher concentrations are observed when the wind is from southerly directions while positive values point northerly directions for high concentrations. The regression parameter related to wind direction (m_3) had positive values and it was statistically significant for the urban site while it was insignificant for the suburban site. The results were consistent with the locations of predominant sources (urban Izmir plume and Aliaga industrial region at north of the suburban and urban sites). It should be noted that the MLR analysis for the urban site is based on a smaller dataset and it may be considered as a limitation on the interpretation of the results from this site.

3.3 Sources of PAHs

PAHs are almost entirely anthropogenic in origin and are major byproducts of the incomplete combustion of all types of OM (e.g., gasoline, diesel, and other fuels) [11, 23]. PAH emission sources are primarily categorized as follows: Heavy oil combustion, natural gas combustion, wood and coal combustion, diesel combustion, and vehicles [24].

The winter/summer total PAH (gas + particle) concentration ratios ranged between 1.4 (CRB) up to 5.9 (BaA), and 3.1 (PHE) up to 11.0 (BaP) for suburban and urban sampling sites, respectively. Higher PAH concentrations observed during wintertime could be attributed to the increasing emissions from residential heating [9, 10, 15, 20, 25–27]. Different ratios for individual compounds indicated that residential heating emissions have a different profile than summertime emissions (Fig. 2).

The concentration ratios of individual PAHs in ambient samples and source emissions are frequently employed as diagnostic tools to identify their origin in ambient air [28, 29]. Recently, in Northern China emission sources of particle-phase PAHs were identified using a diagnostic plot of FLN/(FLN + PY) versus IcdP/(IcdP + BghiP) [30]. Figure 3 illustrates an example of such diagnostics as a plot of FLN/(FLN + PY) against IcdP/(IcdP + BghiP) for particulate PAHs. Both FLN/(FLN + PY) and IcdP/(IcdP + BghiP) are >0.5 in the case of coal/biomass emissions [30]. In Fig. 3, 70% of the urban samples fall in the left-bottom quadrant, indicating predominant influence of petroleum combustion. Samples appearing in the top-right quadrant, suggest coal/biomass combustion emissions. More than 50% of the suburban samples also fall in the left-bottom quadrant, indicating significant influence of petroleum combustion (vehicular emissions). However, some of the suburban samples fall in the left-top and right-top quadrants suggesting that coal/biomass combustion is also a major PAH source at this site.

Li and Kamens [31] observed that the ratio of BaA/BaP was 0.5 for gasoline exhaust and 1.0 for both diesel exhaust and wood combustion. In the present study, the BaA/BaP ratios were significantly higher for winter (1.05) than summer (0.70) at suburban site. These results indicated that, in addition to traffic emissions, wood and coal combustions are the major PAH sources in winter at the
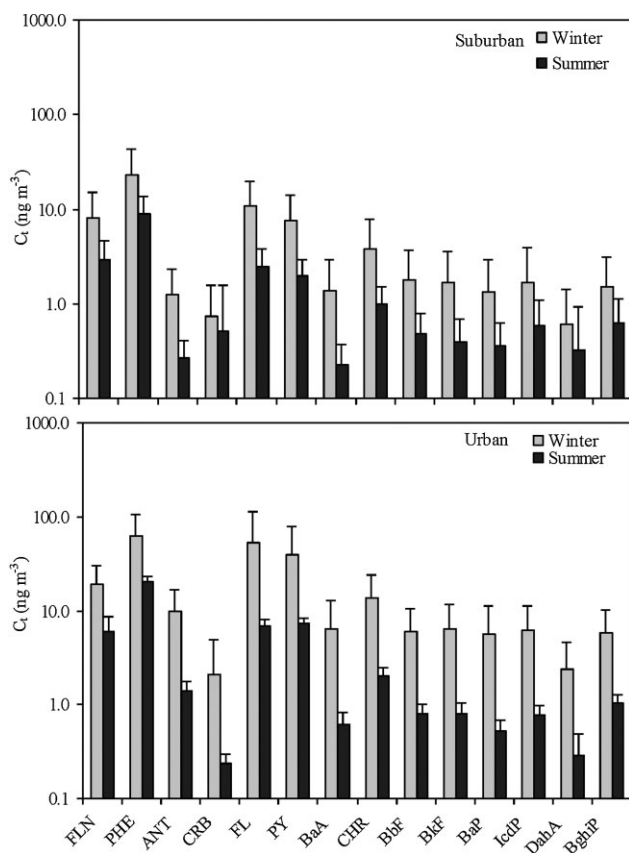
Figure 2. Seasonal variation of individual PAH concentrations in this study. Error bars are 1 SD.

suburban site. In summer, traffic emissions dominated at this site. Many other diagnostic ratios for PAHs are used to identify the potential emission sources at different sites. The diagnostic ratios calculated in this study and reported ones by other studies are compared in Tab. 4. In summary, although may be prone to some errors, the diagnostic plot and diagnostic PAH ratios approaches suggested that traffic emissions (petroleum combustion) were the
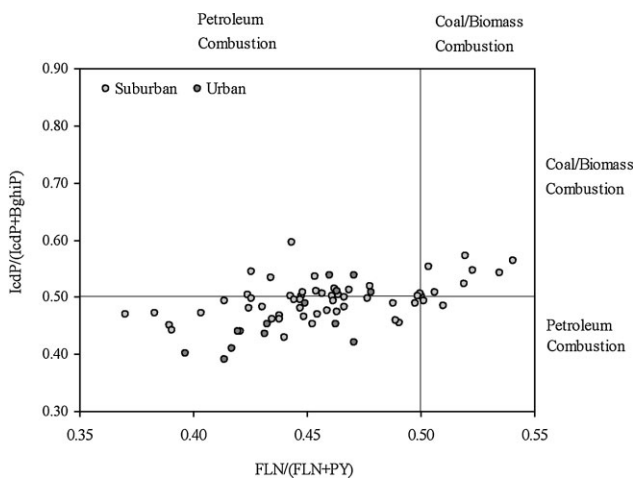
Figure 3. Plot of FLN/(FLN + PYR) against IcdP/(IcdP + BghiP) for PAH source diagnostics. Two dashed lines represent the thresholds for petroleum combustion and coal/biomass burning.

dominant PAH sources at all sites for both seasons. During winter, residential heating was also a possible significant PAH source at all sites.

3.4 Gas–particle partitioning

Partitioning of atmospheric organic compounds between the gas and particle-phases is parameterized using the gas/particle partition coefficient, K_P (m^3 µg^{-1}) [33]:

$$K_P = \frac{C_P/C_{TSP}}{C_g} \tag{2}$$

where C_P and C_g are the organic compound concentrations in the particle and gas-phases, respectively (ng m^{-3}), and C_{TSP} is the concentration of TSP in the air (µg m^{-3}).

The octanol–air partitioning coefficient (K_{OA}) can be used to predict K_P with the assumption of predominant distribution process is absorption [33]. The relationship between K_P and K_{OA} is:

$$K_P = \frac{(f_{OM}MW_{OCT}\zeta_{OCT})K_{OA}}{\rho_{OCT}MW_{OM}\zeta_{OM}10^{12}} \tag{3}$$

where f_{OM} is the fraction of OM phase on TSP, MW_{OCT} and MW_{OM} are the mean molecular weights of octanol and the OM phase (g mol^{-1}), ρ_{OCT} the density of octanol (0.820 kg L^{-1}), ζ_{OCT} the activity coefficient of the absorbing compound in octanol, and ζ_{OM} is the activity coefficient of the compound in the OM phase. With the assumptions that ζ_{OCT}/ζ_{OM} and $MW_{OCT}/MW_{OM} = 1$, Eq. (3) can be written as:

$$\log K_P = \log K_{OA} + \log f_{OM} - 11.91 \tag{4}$$

K_{OA} values were calculated as a function temperature using:

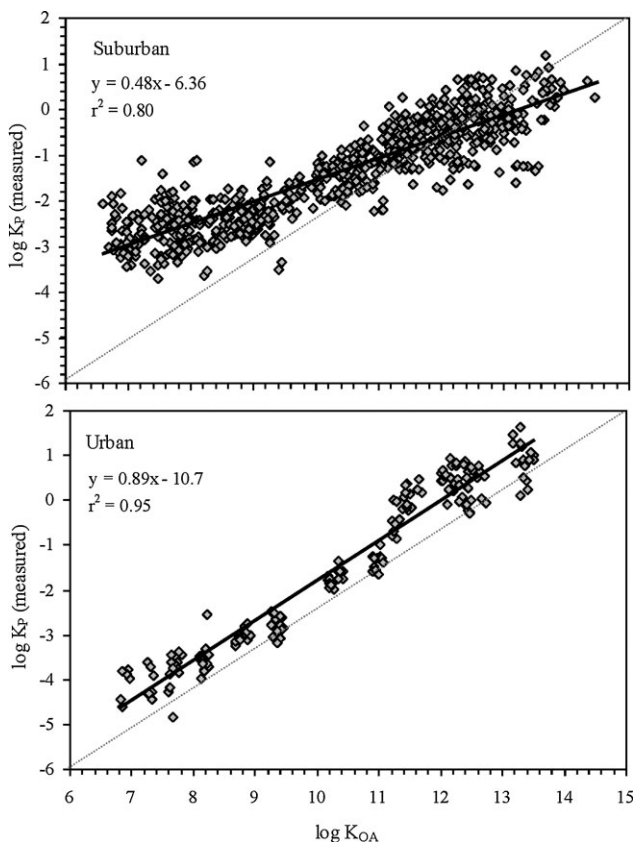$$\log K_{OA} = A + \frac{B}{T} \tag{5}$$

where A is the intercept and B is slope of the temperature regressions given by Odabasi et al. [34] and T is in K.

The experimental gas–particle partition coefficients (K_P) for individual PAHs were calculated using Eq. (2). The relationship between K_P and K_{OA} is expressed using Eq. (4). Plots of $\log K_P$ versus $\log K_{OA}$ have been used in field and laboratory studies to evaluate the gas–particle partitioning of POPs. A good correlation between $\log K_P$ and $\log K_{OA}$ and a slope near 1 indicates that octanol is a good surrogate for the partitioning of POPs into aerosol OM [22]. Figure 4 is a plot of $\log K_P$ (m^3 ng^{-1}) measured at suburban and urban sites versus $\log K_{OA}$. For the plot containing all data, K_P and K_{OA} correlated well ($r^2 = 0.80$–0.95). The regression parameters, m and b were 0.48 and 6.36 for suburban and 0.89 and 10.7 for urban sites, respectively. For individual samples, K_P and K_{OA} were also showed a good correlation ($r^2 = 0.72$–0.97 and 0.94–0.98 for suburban and urban sites). The slope values (m) for suburban and urban sites ranged between 0.22–0.74 and 0.74–1.01, respectively. The variation of slope values for suburban and urban sites suggests that atmospheric particles for different sites might have different sorbing properties. Good correlation between $\log K_P$ and $\log K_{OA}$ suggests that K_{OA} is a useful predictor for the partitioning of PAHs into aerosol OM. Even though strong correlations were observed between $\log K_P$ and $\log K_{OA}$, some of the previously reported slopes were significantly different than 1. As a result of the plots of $\log K_P$ and $\log K_{OA}$, the slope values of 0.45–0.99 for OCPs [22], 0.79, 0.99, 0.74, and 0.65 for PAHs, OCPs, PCBs, and PCNs

Table 4. Diagnostic ratios for ambient air PAHs in this study and previously reported ones for major emission sources

Diagnostic ratios (this study)	Values (winter/summer)		Sources (literature)			
	Suburban	Urban	Gasoline	Diesel	Coal	Wood
BaA/CHR	0.33/0.24	0.43/0.30	0.28−1.2[a] 0.47−0.59[b]	0.17−0.36[a]	1.0−1.2[a] 1.05−1.17[b]	0.66−0.92[b]
BaA/(BaA + CHR)	0.24/0.19	0.30/0.23	0.22−0.55[c),d]	0.38−0.64[c),d]	–	0.43[d]
BaP/BgiP	0.84/0.61	0.85/0.48	0.3−0.4[a]	0.46−0.81[a]	0.9−6.6	–
IcdP/BghiP	1.02/0.91	0.98/0.74	0.27−0.4[b] <0.4[e]	1[b),e]	1.06−1.12[b]	0.23−0.33[b]
IcdP/(IcdP + BghiP)	0.50/0.47	0.49/0.43	0.21−0.22[c),d] 0.18[b]	0.35−0.70[c),b),d),e]	0.56[e]	0.62[d),e]
BbF/BkF	1.08/1.37	0.94/0.99	1.07−1.45[b]	>0.5[e]	3.53−3.87[b]	0.76−1.08[b]
PHE/ANT	20.50/36.57	7.29/15.01	3.4−8[a]	7.6−8.8[a]	3[a]	–
FLN/(FLN + PY)	0.51/0.58	0.38/0.44	0.40[b),d] <0.5[e]	0.60−0.70[b),d] >0.5[e]	–	0.74[b]
FL/(FL + PY)	0.59/0.54	0.55/0.49	0.40[c]	0.60−0.70[c]	–	–
BghiP/BaP	1.25/1.70	1.33/2.11	2.5−3.3[d]	1.2−2.2[d]	–	–
BaP/(BaP + CHR)	0.24/0.25	0.27/0.20	0.73[c]	0.5[e]	–	–
PY/BaP	8.65/6.61	8.26/14.74	~1[e]	~10[e]	–	–

a) [32].
b) [21].
c) [29].
d) [28].
e) [23].

unity slope may further indicate that atmospheric particles have sorbing properties different from that of octanol.

Strong association of PAHs with soot particles in soot−water systems suggests that besides absorption, adsorption partitioning could also be an important sorption mechanism in the atmosphere. Therefore, the following equation for the overall gas−particle partition coefficient that accounts for both OM absorption and soot carbon adsorption was derived by Dachs and Eisenreich [39]:

$$K_P = [(f_{OM}MW_{OCT}\zeta_{OCT})K_{OA}/(\rho_{OCT}MW_{OM}\zeta_{OM}10^{12})]$$
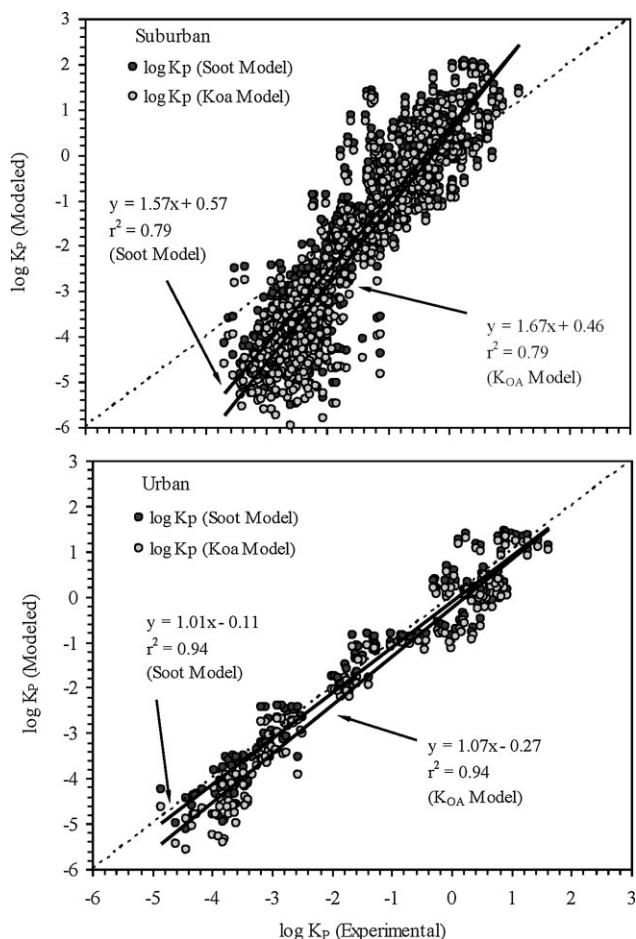$$+ [(f_{EC}a_{EC})K_{SA}/a_{AC}10^{12}] \tag{6}$$

where f_{EC} is the fraction of elemental carbon in the aerosol, a_{EC} and a_{AC} are the specific surface areas of elemental carbon and organic carbon, respectively, and K_{SA} is the soot−air partition coefficient. Elemental carbon and octanol are the surrogates for the soot carbon in adsorptive partitioning, and OM in absorptive partitioning, respectively. The a_{EC} value ($62.7\,m^2\,g^{-1}$) was taken from a recent study by Jonker and Koelmans [40]. The average OM contents of PM measured in this study were 53 ± 20 and $49 \pm 10\%$ for suburban and urban sites, respectively. Recently, OM contents were reported to be 53% [22] and 53.5−62.1% [41] in the Izmir area. The values measured in the present study were similar to these, however, they were higher than those typically assumed in modeling studies (10−20%) [22, 35]. It was assumed that $a_{EC}/a_{AC} = 1$, $f_{OM} = 1.6 f_{OC}$, and $f_{OC}/f_{EC} = 3$ where f_{OC} is the fraction of total organic carbon [39, 42].

Dachs et al. [43] have suggested that the thermodynamics-based model recently reported by van Noort [44] can be used to estimate K_{SA} values for PAHs as a function of supercooled liquid vapor pressure (P_L, Pa) and elemental carbon specific surface area (a_{EC}, $m^2\,g^{-1}$):

$$\log K_{SA} = -0.85 \log P_L + 8.94 - \log(998/\alpha_{EC}) \tag{7}$$

P_L values as a function of temperature can be calculated using:

$$\log P_L(Pa) = m_L T^{-1} + b_L \tag{8}$$

Figure 4. Plots of log K_P ($m^3\,ng^{-1}$) measured at suburban and urban sampling sites versus logK_{OA}. The dashed diagonal line represents a 1:1 relationship (equilibrium).

were reported, respectively [33, 35−37]. Goss and Schwarzenbach [38] have suggested that the slope might deviate from 1 for equilibrium partitioning when logK_P is plotted versus logK_{OA}. Deviations from a

Figure 5. Comparison of the measured and predicted K_P values by two partitioning models. The dashed diagonal line represents a 1:1 relationship.

where b_L is the intercept and m_L is the slope of the temperature regressions [35].

The atmospheric PAH concentrations measured in this study were used to investigate the partitioning of PAHs between particle and gas-phase. Modeled K_P values were calculated using Eq. (4) for absorptive partitioning and Eq. (6) for both absorptive and adsorptive partitioning [34]. The modeled K_P values for absorptive partitioning and for both absorptive and adsorptive partitioning were compared to the measured ones in Fig. 5. The correlations between experimental and modeled K_P values were significant ($r^2 = 0.79$ and 0.94 for suburban and urban sites, respectively, $p < 0.01$). Octanol-based absorptive partitioning model predicted lower partition coefficients especially for relatively volatile PAHs. However, overall there is a relatively good agreement between the measured K_P and soot-based model predictions. Ratios of measured/modeled partition coefficients ranged between 0.15 (BghiP) up to 651 (FLN) (80 ± 394, average ± SD) and 1.2 (CHR) up to 15.5 (FLN) (4.5 ± 6.0, average ± SD) for the K_{OA} model in suburban and urban sites, respectively. The soot model predictions were relatively better and measured to modeled ratios ranged between 0.11 (BghiP) up to 232 (FLN) (30 ± 141, average ± SD) and 0.6 (CHR) up to 5.6 (FLN) (2.3 ± 2.7, average ± SD) for suburban and urban sites, respectively. Recent studies reported that the soot-based model showed a good predictability at an urban site (Chicago, IL) but underestimated the

values at a rural site (Eagle Harbor) by an order of magnitude [45, 46]. It was suggested that characterizing atmospheric soot, determining the temperature dependence of soot–air partitioning, and quantifying the exchangeable fraction of each PAH on aerosols will help to explain the differences between predicted and observed partition coefficients [46].

It was observed that gas–particle partitioning of PAHs was different for suburban and urban samples. This was evident by the more shallow slopes obtained from the plots of $\log K_P$ versus $\log K_{OA}$ at the suburban site compared to those for urban sites. Recently, Vardar et al. [45] have reported steeper slopes for lake samples relative to the land samples in Chicago. It was suggested that the observed differences between the lake and land samples may be due to the different properties of particles (i.e., aged particles as a result of longer residence time for lake samples), non-exchangeability and differences in activity coefficients of PAHs. Similarly, in the present study urban samples had steeper slopes than the suburban samples. However, unlike the Chicago samples that had different levels of TSP concentrations (i.e., low for lake and higher for land samples) suburban and urban samples of the present study had similar average TSP concentrations (~ 70–$80\,\mu g\,m^{-3}$, respectively). Previous experimental studies have shown that a greater fraction of the higher molecular weight PAHs are associated with fine particles relative to the lower molecular weight compounds [26, 47, 48]. Recent studies indicated that the contribution of wind-entrained soil particles to atmospheric coarse PM is significant at the suburban site [49, 50]. The contribution of local soil to the coarse PM increases especially the particle-phase concentrations of low molecular weight PAHs. This increase in particle-phase concentration will result in larger K_P values especially for low molecular weight PAHs (Eq. 2) and consequently more shallow slopes for $\log K_P$ versus $\log K_{OA}$ plots (Fig. 4).

4 Conclusions

Ambient air PAH samples were collected at a suburban ($n = 63$) and at an urban site ($n = 14$) in Izmir, Turkey. Higher ambient PAH concentrations were measured in the gas-phase and $\sum_{14}$PAH concentrations were dominated by lower molecular weight PAHs. MLR analysis indicated that the meteorological parameters were effective on the measured ambient PAH concentrations. Emission sources of particle-phase PAHs were investigated using diagnostic plots and diagnostic ratios. These approaches have indicated that traffic emissions (petroleum combustion) were the dominant PAH sources at both sites for summer and winter seasons.

Experimental gas–particle partition coefficients (K_P) were compared to the predictions of octanol–air (K_{OA}) and soot–air (K_{SA}) partition coefficient models. Octanol-based absorptive partitioning model predicted lower partition coefficients especially for relatively volatile PAHs. However, overall there was a relatively good agreement between the measured K_P and soot-based model predictions.

The authors have declared no conflict of interest.

References

[1] R. Dabestani, I. N. Ivanov, A Complication of Physical, Spectroscopic and Photophysical Properties of Polycyclic Aromatic Hydrocarbons, *Photochem. Photobiol.* **1999**, *70 (1)*, 10–34.

[2] M. Odabasi, *PhD Thesis*, Illinois Institute of Technology, Chicago **1998**.

[3] R. Lohmann, G. Lammel, Adsorptive and Absorptive Contributions to the Gas–Particle Partitioning of Polycyclic Aromatic Hydrocarbons: State of Knowledge and Recommended Parametrization for Modeling, *Environ. Sci. Technol.* 2004, *38*, 3793–3803.

[4] C. J. Halsall, P. J. Coleman, B. J. Davis, V. Burnett, K. S. Waterhouse, P. Harding-Jones, K. C. Jones, Polycyclic Aromatic Hydrocarbons in U.K. Urban Air, *Environ. Sci. Technol.* 1994, *28*, 2380–2386.

[5] M. Odabasi, N. Vardar, A. Sofuoglu, Y. Tasdemir, T. M. Holsen, Polycyclic Aromatic Hydrocarbons (PAHs) in Chicago Air, *Sci. Total Environ.* 1999, *227*, 57–67.

[6] J. Dachs, T. R. Glenn IV, C. L. Gigliotti, P. Brunciak, L. A. Totten, E. D. Nelson, T. P. Franz, S. J. Eisenreich, Processes Driving the Short-Term Variability of Polycyclic Aromatic Hydrocarbons in the Baltimore and Northern Chesapeake Bay Atmosphere, USA, *Atmos. Environ.* 2002, *36*, 2281–2295.

[7] C. L. Gigliotti, P. A. Brunciak, J. Dachs, T. R. Glenn IV, E. D. Nelson, L. A. Totten, S. J. Eisenreich, Air–Water Exchange of Polycyclic Aromatic Hydrocarbons in the New York, New Jersey, USA, Harbor Estuary, *Environ. Toxicol. Chem.* 2002, *21*, 235–244.

[8] M. Mandalakis, M. Tsapakis, A. Tsoga, E. G. Stephanou, Gas–Particle Concentrations and Distribution of Aliphatic Hydrocarbons, PAHs, PCBs and PCDD/Fs in the Atmosphere of Athens (Greece), *Atmos. Environ.* 2002, *36*, 4023–4035.

[9] S. S. Park, Y. J. Kim, C. H. Kang, Atmospheric Polycyclic Aromatic Hydrocarbons in Seoul, Korea, *Atmos. Environ.* 2002, *36*, 2917–2924.

[10] T. Ohura, T. Amagai, M. Fusaya, H. Matsushita, Spatial Distributions and Profiles of Atmospheric Polycyclic Aromatic Hydrocarbons in Two Industrial Cities in Japan, *Environ. Sci. Technol.* 2004, *38*, 49–55.

[11] G. C. Fang, K. F. Chang, C. Lu, H. Bai, Estimation of PAHs Dry Deposition and BaP Toxic Equivalency Factors (TEFs) Study at Urban, Industry Park and Rural Sampling Sites in Central Taiwan, Taichung, *Chemosphere* 2004, *55*, 787–796.

[12] M. Possanzini, V. Di Palo, P. Gigliucci, M. C. T. M. C. Tomasi Sciano, A. Cecinato, Determination of Phase-Distributed PAH in Rome Ambient Air by Denuder/GC-MS Method, *Atmos. Environ.* 2004, *38*, 1727–1734.

[13] M. Tsapakis, E. G. Stephanou, Occurrence of Gaseous and Particulate Polycyclic Aromatic Hydrocarbons in the Urban Atmosphere: Study of Sources and Ambient Temperature Effect on the Gas/Particle Concentration and Distribution, *Environ. Pollut.* 2005, *133*, 147–156.

[14] Y. Tasdemir, F. Esen, Urban Air PAHs: Concentrations, Temporal Changes and Gas/Particle Partitioning at a Traffic Site in Turkey, *Atmos. Res.* 2007, *84*, 1–12.

[15] A. Bozlaker, A. Muezzinoglu, M. Odabasi, Atmospheric Concentrations, Dry Deposition and Air–Soil Exchange of Polycyclic Aromatic Hydrocarbons (PAHs) in an Industrial Region in Turkey, *J. Hazard. Mater.* 2008, *153*, 1093–1102.

[16] M. Akyuz, H. Cabuk, Gas–Particle Partitioning and Seasonal Variation of Polycyclic Aromatic Hydrocarbons in the Atmosphere of Zonguldak, Turkey, *Sci. Total Environ.* 2010, *408*, 5550–5558.

[17] S. Ozcan, M. E. Aydin, Polycyclic Aromatic Hydrocarbons, Polychlorinated Biphenyls and Organochlorine Pesticides in Urban Air of Konya, Turkey, *Atmos. Res.* 2009, *93*, 715–722.

[18] F. Esen, S. S. Cindoruk, Y. Tasdemir, Ambient Concentrations and Gas/Particle Partitioning of Polycyclic Aromatic Hydrocarbons in an Urban Site in Turkey, *Environ. Forensics* 2006, *7*, 303–312.

[19] F. Esen, Y. Tasdemir, N. Vardar, Atmospheric Concentrations of PAHs, Their Possible Sources and Gas-to-Particle Partitioning at a Residential Site of Bursa, Turkey, *Atmos. Res.* 2008, *88*, 243–255.

[20] B. Gevao, J. Hamilton-Taylor, K. C. Jones, Polychlorinated Biphenyl and Polycyclic Aromatic Hydrocarbon Deposition to and Exchange at the Air–Water Interface of Esthwaite Water, a Small Lake in Cumbria, UK, *Environ. Pollut.* 1998, *102*, 63–75.

[21] G. C. Fang, C. N. Chang, Y. S. Wu, P. P. C. Fu, I. L. Yang, M. H. Chen, Characterization, Identification of Ambient Air and Road Dust Polycyclic Aromatic Hydrocarbons in Central Taiwan, Taichung, *Sci. Total Environ.* 2004, *327*, 135–146.

[22] A. Sofuoglu, E. Cetin, S. S. Bozacioglu, G. D. Sener, M. Odabasi, Short-Term Variation in Ambient Concentrations and Gas/Particle Partitioning of Organochlorine Pesticides in Izmir, Turkey, *Atmos. Environ.* 2004, *38*, 4483–4493.

[23] K. Ravindra, R. Sokhi, R. Van Grieken, Atmospheric Polycyclic Aromatic Hydrocarbons: Source Attribution Emission Factors and Regulation, *Atmos. Environ.* 2008, *42*, 2895–2921.

[24] H. H. Yang, C. M. Chen, Emission Inventory and Sources of Polycyclic Aromatic Hydrocarbons in the Atmosphere at a Suburban Area in Taiwan, *Chemosphere* 2004, *56*, 879–887.

[25] G. Kiss, Z. Varga-Puchony, G. Rohrbacher, J. Hlavay, Distribution of Polycyclic Aromatic Hydrocarbons on Atmospheric Aerosol Particles of Different Sizes, *Atmos. Res.* 1998, *46*, 253–261.

[26] S. Y. Bae, S. M. Yi, Y. P. Kim, Temporal and Spatial Variations of the Particle Size Distribution of PAHs and Their Dry Deposition Fluxes in Korea, *Atmos. Environ.* 2002, *36*, 5491–5500.

[27] J. Schnelle-Kreis, M. Sklorz, A. Peters, J. Cyrys, R. Zimmermann, Analysis of Particle Associated Semi-Volatile Aromatic and Aliphatic Hydrocarbons in Urban Particulate Matter on a Daily Basis, *Atmos. Environ.* 2005, *39*, 7702–7714.

[28] E. Manoli, A. Kouras, C. Samara, Profile Analysis of Ambient and Source Emitted Particle-Bound Polycyclic Aromatic Hydrocarbons from Three Sites in Northern Greece, *Chemosphere* 2004, *56*, 867–878.

[29] N. Tang, T. Hattori, R. Taga, K. Igarashi, X. Yang, K. Tamura, H. Kakimoto, et al., Polycyclic Aromatic Hydrocarbons and Nitropolycyclic Aromatic Hydrocarbons in Urban Air Particulates and Their Relationship to Emission Sources in the Pan-Japan Sea Countries, *Atmos. Environ.* 2005, *39*, 5817–5826.

[30] S. Liu, S. Tao, W. Liu, Y. Liu, H. Dou, J. Zhao, L. Wang, et al., Atmospheric Polycyclic Aromatic Hydrocarbons in North China: A Winter-Time Study, *Environ. Sci. Technol.* 2007, *41*, 8256–8261.

[31] C. Li, R. Kamens, The Use of Polycyclic Aromatic Hydrocarbons as Source Signatures in Receptor Modeling, *Atmos. Environ.* 1993, *27A*, 523–532.

[32] M. F. Simcik, S. J. Eisenreich, P. J. Lioy, Source Apportionment and Source/Sink Relationships of PAHs in Coastal Atmosphere of Chicago and Lake Michigan, *Atmos. Environ.* 1999, *33*, 5071–5079.

[33] T. Harner, T. F. Bidleman, Octanol–Air Partition Coefficient for Describing Particle/Gas Partitioning of Aromatic Compounds in Urban Air, *Environ. Sci. Technol.* 1998, *32*, 1494–1502.

[34] M. Odabasi, E. Cetin, A. Sofuoglu, Determination of Octanol–Air Partition Coefficients and Supercooled Liquid Vapor Pressures of PAHs as a Function of Temperature: Application to Gas/Particle Partitioning in an Urban Atmosphere, *Atmos. Environ.* 2006, *40*, 6615–6625.

[35] A. Finizio, D. Mackay, T. F. Bidleman, T. Harner, Octanol–Air Partition Coefficient as a Predictor of Partitioning of Semivolatile Organic Chemicals, *Atmos. Environ.* 1997, *31*, 2289–2296.

[36] R. L. Falconer, T. Harner, Comparison of the Octanol–Air Partition Coefficient and Liquid Phase Vapor Pressure as Descriptors for Particle/Gas Partitioning Using Laboratory and Field Data for PCBs and PCNs, *Atmos. Environ.* 2000, *34*, 4043–4046.

[37] M. Shoeib, T. Harner, Using Measured Ocatanol–Air Partition Coefficients to Explain Environmental Partitioning of Organochlorine Pesticides, *Environ. Sci. Technol.* 2002, *21*, 984–990.

[38] K. Goss, R. P. Schwarzenbach, Gas/Solid and Gas/Liquid Partitioning of Organic Compounds: Critical Evaluation of the Interpretation of Equilibrium Constants, *Environ. Sci. Technol.* 1998, *32*, 2025–2032.

[39] J. Dachs, S. J. Eisenreich, Adsorption onto Aerosol Soot Carbon Dominates Gas–Particle Partitioning of Polycyclic Aromatic Hydrocarbons, *Environ. Sci. Technol.* 2000, *34*, 3690–3697.

[40] M. T. Jonker, A. A. Koelmans, Sorption of Polycyclic Aromatic Hydrocarbons and Polychlorinated Biphenyls to Soot and Soot-Like Materials in the Aqueous Environment: Mechanistic Considerations, *Environ. Sci. Technol.* 2002, *36*, 3725–3734.

[41] B. Cetin, M. Odabasi, Atmospheric Concentrations and Phase Partitioning of Polybrominated Diphenyl Ethers (PBDEs) in Izmir, Turkey, *Chemosphere* 2008, *71*, 1067–1078.

[42] S. Ribes, B. Van Drooge, J. Dachs, Ä. Gustafsson, J. O. Grimalt, Influence of Soot Carbon on the Soil–Air Partitioning of Polycyclic Aromatic Hydrocarbons, *Environ. Sci. Technol.* **2003**, *37*, 2675–2680.

[43] J. Dachs, S. Ribes, B. V. Drooge, J. Grimalt, Response to the Comment on "Influence of Soot Carbon on the Soil–Air Partitioning of Polycyclic Aromatic Hydrocarbons", *Environ. Sci. Technol.* **2004**, *38*, 1624–1625.

[44] P. C. M. van Noort, A Thermodynamics-Based Estimation Model for Adsorption of Organic Compounds by Carbonaceous Materials in Environmental Sorbents, *Environ. Toxicol. Chem.* **2003**, *22*, 1179–1188.

[45] N. Vardar, Y. Tasdemir, M. Odabasi, K. E. Noll, Characterization of Atmospheric Concentrations and Partitioning of PAHs in the Chicago Atmosphere, *Sci. Total Environ.* **2004**, *327*, 163–174.

[46] E. Galarneau, T. F. Bidleman, P. Blanchard, Seasonality and Interspecies Differences in Particle/Gas Partitioning of PAHs Observed by the Integrated Atmospheric Deposition Network (IADN), *Atmos. Environ.* **2006**, *40*, 182–197.

[47] M. Odabasi, A. Sofuoglu, N. Vardar, Y. Tasdemir, T. M. Holsen, Measurement of Dry Deposition and Air–Water Exchange of Polycyclic Aromatic Hydrocarbons with the Water Surface Sampler, *Environ. Sci. Technol.* **1999**, *33*, 426–434.

[48] Y. Tasdemir, F. Esen, Dry Deposition Fluxes and Deposition Velocities of PAHs at an Urban Site in Turkey, *Atmos. Environ.* **2007**, *41*, 1288–1301.

[49] S. Yatkin, A. Bayram, Elemental Composition and Sources of Particulate Matter in the Ambient Air of a Metropolitan City, *Atmos. Res.* **2007**, *85*, 126–139.

[50] S. Yatkin, A. Bayram, Source Apportionment of PM10 and PM2.5 Using Positive Matrix Factorization and Chemical Mass Balance in Izmir, Turkey, *Sci. Total Environ.* **2008**, *390*, 109–123.